Bauyrzhan RAKHADILOV[*], Sherzod KURBANBEKOV[*], Arman MINIYAZOV[*]

THE INFLUENCE OF ELECTROLYTIC-PLASMA NITRIDING ON THE STRUCTURE AND TRIBOLOGICAL PROPERTIES OF HIGH-SPEED STEELS

WPŁYW AZOTOWANIA ELEKTROLITYCZNO--PLAZMOWEGO NA STRUKTURĘ I WŁASNOŚCI TRIBOLOGICZNE STALI SZYBKOTNĄCYCH

Key words:

electrolytic-plasma nitriding, high-speed stel, phase composition, wear resistance

Słowa kluczowe:

azotowanie elektrolityczno-plazmowe, stal szybkotnąca, skład fazowy, odporność na zużywanie

Summary

The effect of the electrolytic-plasma nitriding on a structure and tribological properties of the R9, R6M5 and R18 type high-speed steels (HSS) has been investigated. It is shown that, after this treatment at the temperature of 550°C, a nitrided layer containing the Fe_4N monophase nitride (γ'-phase) is formed.

[*] Branch Institute of Atomic Energy RSE NNC RK Kurchatov, Kazakhstan, e-mail: bor1988@mail.ru

This nitrided layer has a high wear resistance with wear intensity reduded to 1/6th of the figure for non-treated samples.

INTRODUCTION

The operability of cutting tools depends on the state of the surface layer **[L. 1]**. To increase the hardness, strength, and durability, different thermal and thermal-chemical treatments are used. Recently, there has been an increase in the development and application of plasma nitriding that overcome the shortcomings of traditional methods of nitriding **[L. 2]**. Plasma nitriding provides the formation of a nitrided layer with a specified structure on the surface of processed parts. This increases tool life and its heat resistance. A nitrided surface of tools with a low friction coefficient and improved anti-friction properties provides easier shaving removal and prevents its pickup on the cutting edges and holes, which helps to increase the feed and cutting speed **[L. 3–5]**.

Currently, a fire-intensifying process of diffusion saturation **[L. 6]** is a very promising direction in increasing the productivity of the process of plasma nitriding. One of the modern methods of plasma nitriding that will help reduce overall processing time and significantly improve the wear resistance of structural and tool steels is electrolytic-plasma nitriding **[L. 7]**. Electrolytic-plasma nitriding produces significant changes in the structural-phase state causing changes in the material properties in the thin surface layers due to the physical impacts of ions of high-temperature plasma and electric discharge. During the developing processes of restructuring, structural-phase transformations occur in the conditions far from thermodynamic equilibrium states, and they allow one to obtain modified surface layers with a unique set of physical and mechanical properties **[L. 8]**.

In connection with the above, the purpose of this work is to study the influence of electrolytic-plasma nitriding on the structure-phase states and HSS tribological properties.

MATERIAL AND METHODS OF RESEARCH

The study materials were samples of R6M5, R18, and R9 HSS. The steels chemical composition of is shown in **Table 1**.

For electrolytic-plasma nitriding, samples from R6M5, R18 and R9 steels were used with dimensions 10 x 30 x 30 mm^3 and after standard thermal processing for these steels **[L. 9]**. Regimes of thermal processing are given in **Table 2**.

After thermal processing, the samples were ground and polished. Then the samples were processed by electrolytic-plasma nitriding.

Table 1. Composition of the R9, R6M5 and R18 grade high-speed steels (according to Standard 19265-73)
Tabela 1. Skład stali szybkotnących typu R9, R6M5 i R18 (wg normy 19265-73)

Steel	C	Mn	Si	Cr	W	V	Co	Mo	Ni	Cu	S	P
R9	0.85-0.95	up to 0.50	up to 0.50	3.80-4.40	8.50-9.50	2.30-2.70	up to 0.50	up to 1.00	up to 0.40	-	up to 0.03	up to 0.03
R6M5	0.82-0.9	0.20-0.50	0.20-0.50	3.80-4.40	5.50-6.50	1.70-2.10	up to 0.50	4.80-5.30	up to 0.60	up to 0.25	up to 0.025	up to 0.03
R18	0.73-0.83	0.20-0.50	0.20-0.50	3.80-4.40	17.00-18.50	1.00-1.40	up to 0.50	up to 1.00	up to 0.60	up to 0.25	up to 0.03	up to 0.03

Table 2. Regimes of the thermal processing of samples
Tabela 2. Warunki obróbki cieplnej próbek

Steel	Thermal processing	
	quenching	tempering
R9	from 1230°C in oil	560°C (threefold: duration of each 1 hour, air cooling)
R6M5	from 1230°C in oil	560°C (threefold: duration of each 1 hour, air cooling)
R18	from 1270°C in oil	560°C (threefold: duration of each 1 hour, air cooling)

Electrolytic-plasma nitriding of samples was performed using an experimental industrial installation that has the following main parts: an electrolytic cell, a power supply, an automatic control system, an electrolyte-cooling system, and an electrolyte feed system **[L. 10]**. Descriptions of the electrolytic-plasma nitriding process of the HSS samples are shown in **Figure 1**. The process was carried out in an electrolyte water solution contained 20% of carbamide and 10% of natrium carbonate with an active cathode in the following regime: samples nitriding temperature – 550°C, supplied voltage between anode and sample during heated to nitriding temperature – 320 V, handling at 550°C – 200 V, and nitriding time – 7 minutes.

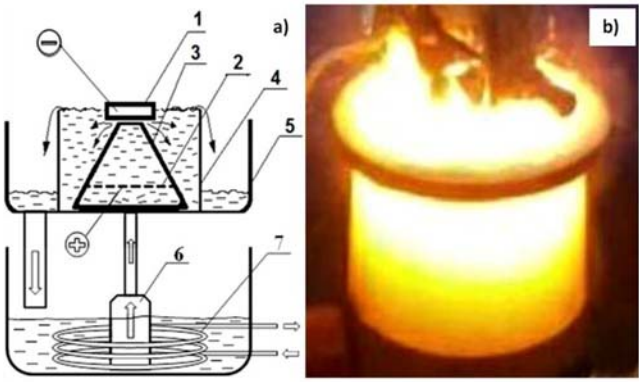

Fig. 1. Process scheme (a) and view of the electrolytic-plasma nitriding of the HSS samples (b): 1 – processed sample (cathode), 2 – stainless steel with holes (anode), 3 – cone shaped barrier, 4 – electrolytic cell, 5 – container, 6 – pump, 7 – heat exchanger

Rys. 1. Schemat procesu (a) i prezentacja azotowania elektrolityczno-plazmowego próbek HSS (b): 1 – obrabiana próbka (katoda), 2 – stal nierdzewna z otworami (anoda), 3 – przegroda stożkowa, 4 – komórka elektrolityczna, 5 – zbiornik, 6 – pompa, 7 – wymiennik ciepła

Metallographic research was conducted on an (ALTAMI-MET-1M) optical microscope. The microstructures of the samples were investigated on a JSM-6390LV scanning electron microscope. The studies on phase composition and the crystal structure of samples were carried out by X-ray diffraction analysis on a D8 ADVANCE diffractometer in CuK_{α}-radiation, using 0.02º step size and a 0.2 s time step. To identify the grain boundaries and particles of the carbide phases, chemical etching of thin sections 4% alcohol solution of nitric acid (the etching 5–7 s) was applied. The microhardnesses of the samples' surface coatings were measured before and after the process using a diamond indenter (PMT-3M Apparatus) under a load of 100 g for 10 s.

The tribological tests for sliding friction were executed using a high-temperature THT-S-BE-0000 Friction (ball/disk) Apparatus **(Figure 2a)**. The small ball with a diameter of 6.0 mm was used as the opposing surface made of certified material, i.e. Al_2O_3. The tests were conducted in ambient conditions (environmental temperature: 30°C, atmospheric pressure: 25.4 Hg, relative humidity: 44.0%) under load of 1 N and linear speed of 2 cm/s, a curvature radius of wear of 5 mm, and a sliding distance of 31.4 m. The number of test cycles for all samples was the same and comprises 1000. The tribological specifications of the modified coating are characterized by wear intensity.

The tests of the samples for wear-resistance were conducted using an experimental apparatus for tests of abrasive wear in rolling contact using a flowing abrasive according to the schema of a roller on a flat surface and to the State Standard of 23.208-79 that corresponds to the ASTM S 6568 American Standard. For testing abrasive friction on an "air cushion" (abrasive

wheel on rubber bonding material), the surfaces of samples were ground and polished to the roughness of Ra = 1.2 μm, and they were cleaned using acetone and dried. The cylindrical rubber roller pressed by a radial surface to the flat surface of the studied sample with a pressure of 22 N at a frequency of 1 s^{-1}. The schema of the apparatus is shown in **Figure 2b**. The rate of the arrival of abrasive parts between the rubber roller and the sample, i.e. to the test zone, was 41–42 g/min. The electrocorundum with abrasive grit of 200…250 μm was used as the abrasive. The wear-resistance of the studied nitrate sample was assessed by means of a comparison of its wear to the wear of a standard sample (non-nitrate sample). The wear was measured by the weight method using an ADV-200 Chemical Balance with an accuracy of 0.0001 g. The samples were weighted every minute and tested every three minutes, the total length of wear sequence was 28.8 m. The samples cleaned with compressed air to removal the remaining sand particles on the probes before measurements were taken.

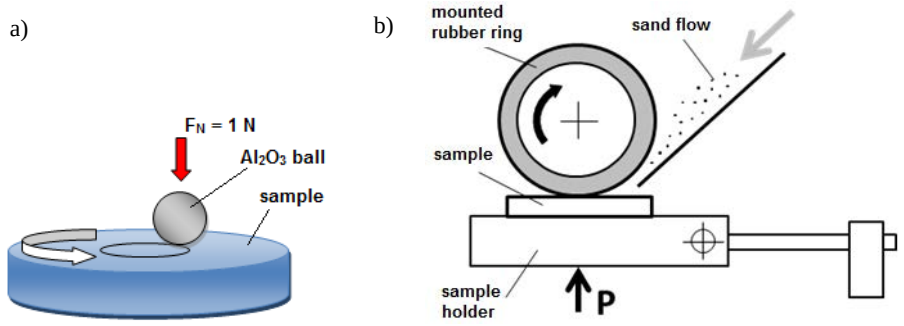

Fig. 2. Arrangements of the test rigs used: a) ball-on-disk tester, b) loose grains abrasion tester

Rys. 2. Konfiguracje zastosowanych urządzeń testowych: a) tester kula–tarcza, b) tester odporności na zużywanie luźnym ścierniwem

RESEARCH RESULTS AND THEIR DISCUSSION

One of the most important properties of the nitrided layer is hardness. Hardness and the thickness of the diffusion layer depend on alloying elements in the material. It is known that, under the same nitriding conditions (temperature and process time), the diffusion layer hardness increases with the increased content of alloying elements, while the diffusion layer thickness decreases **[L. 11]**.

Figure 3 shows the microhardness distribution in the depth of the nitrided layer. A significant increase in the microhardness of the steel surface was evident. The character of the transition zone had a smooth transition from the hardened layer to base material, and the base material's microhardness is not

significantly changed. The nitrided layers microhardness of R9, R6M5, R18 steels were different from each other. This is because the alloying elements are present in various quantities in each type of steel. The R18 steel nitrided layer has a higher hardness when compared to R6M5 and R9, because R18 steel has more nitride-forming elements, such as tungsten.

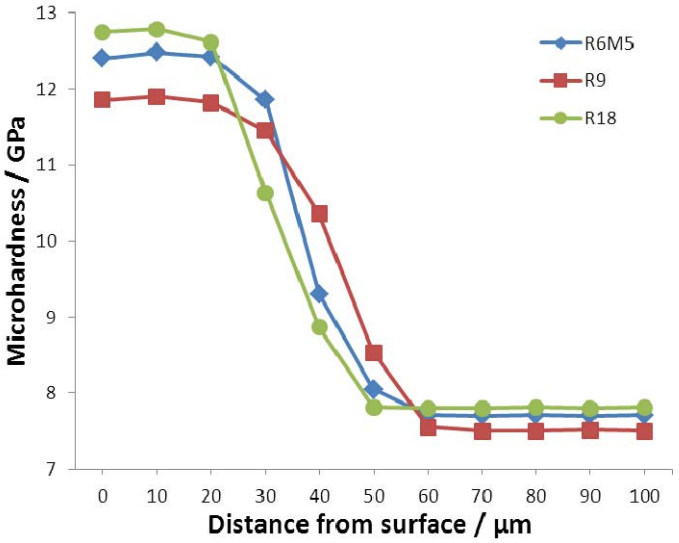

Fig. 3. Microhardness as a function of the distance from surface
Rys. 3. Mikrotwardość w funkcji odległości od powierzchni

Microstructure steels after electrolytic-plasma nitriding are shown in **Figure 4**. The surface is a dark-etched nitrided layer indicating the presents of nitrogen martensite. The dark-etching area is blended into basis. The thickness of R9, R6M5, R18 steels nitrided layers are 45 µm, 40 µm, and 35 µm, respectively.

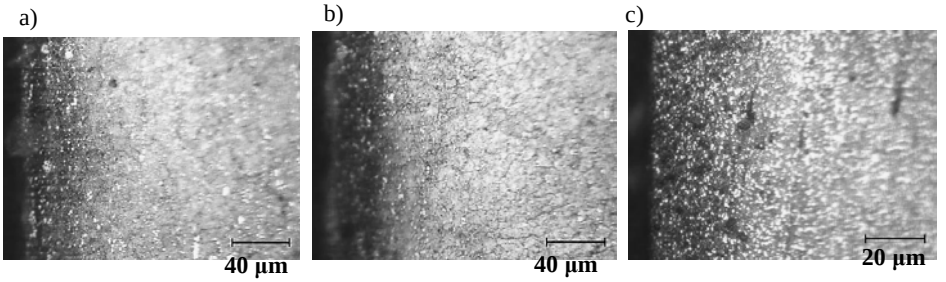

Fig. 4. Microstructure of the HSS nitrided layers: a) R9 steel, b) R6M6 steel, R18 steel
Rys. 4. Microstruktura azotowanych warstw HSS: a) stal R9, b) stal R6M6, stal R18

Figure 5 shows the SEM images of R6M5 steel surface before and after nitriding. Tests determined that fine inclusions with an average size ~0.1 μm are formed on HSS surface during electrolytic-plasma nitriding. It is assumed that these fine inclusions are fine nitrides of alloying elements. Therefore, it is quite possible formation of fine nitrides of alloying elements, in particular chromium, while nitriding HSSs **[L. 12]**.

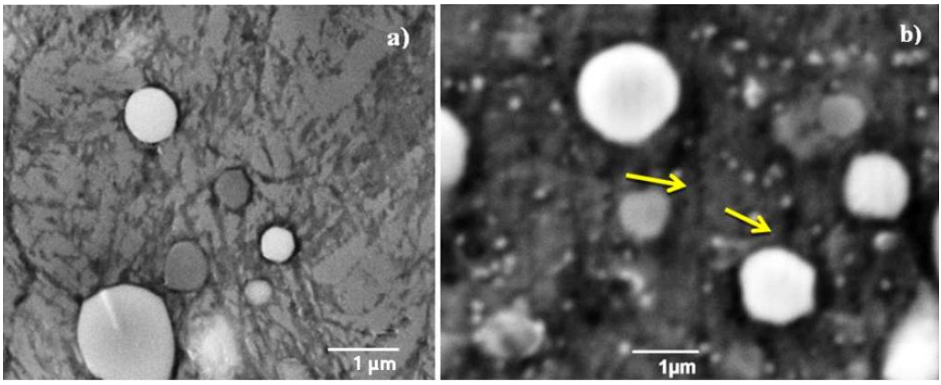

Fig. 5. The SEM images of the samples of R6M5 surface after electrolytic-plasma nitriding
Rys. 5. Obrazy SEM powierzchni próbek R6M5 po azotowaniu elektrolityczno-plazmowym

Figure 6 shows the diffraction patterns of R9, R6M5, and R18 HSS. X-ray analysis showed that, after thermal processing, martensite (α-phase) and carbides M6C and MC are present in the P9, R6M5 and R18 steels' structure. After nitriding, diffractograms indicated the Fe_4N interference line phase **(Figure 4)**. A broadening, intensity decrease, and a shift towards Bragg's smaller corners of interference lines (110) (211) α-phase were observed, which indicates the formation of a solid solution of nitrogen the area of the internal nitriding **[L. 13]**. The X-ray study revealed alloying elements in the nitride phases, which were probably due to their low concentration and small size. Perhaps this is also connected with formation of fine nitrides distribution on the layers, but they cannot be identified with the existing sensitivity of X-ray phase analysis.

On the basis of X-ray analysis, one can argue that the high hardness of the nitrided layer of HSS is associated with the formation of γ'-phase and nitrogen martensite.

Therefore, the main advantage of nitriding with electrolytic-plasma exposure is that it is possible to obtain a diffusion strengthened layer with Fe_4N monophasic nitride (γ'-phase), unlike gas nitriding in ammonia, where nitride layer consists of two γ'- and e-phases, which is the source of internal stresses on the phase boundary and causes fragility and peeling of the hardened layer of

cutting tools during operation **[L. 14]**. The influence of the diffusion layer of nitrogen martensite in the surface layers will positively influence the performance properties of the cutting tool from R6M5 HSS. As nitrides of iron have greater capacity compared with iron **[L. 15]**. This creates favourable conditions for the prevention of temperature flares on the cutting tool surface.

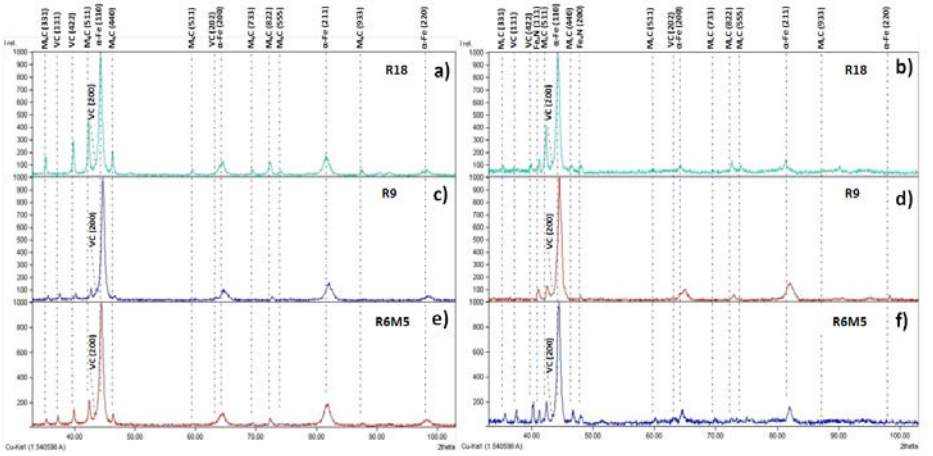

Fig. 6. Diffractograms of the R18, R9 and R6M6 (from top to bottom) steels before (a, c, e) and after (b, d, f) electrolytic-plasma nitriding

Rys. 6. Dyfraktogramy stali R18, R9 i R6M6 (od góry do dołu) przed (a, c, e) oraz po (b, d, f) azotowaniu elektrolityczno-plazmowym

Thus, the X-ray showed that the main carbides in the studied steels are M_6C and MC. It was determined that that carbide type M_6C optimally combined with the Fe_3W_3C phase, and carbide type MC corresponds to the VC phase. Quantitative X-ray analysis showed that there was no marked change in the content of carbide phases after nitriding. The content of Fe_4N nitride (γ'-phase) in R9, R6M5, R18 steels are 5.5, 3.9, and 3.7, respectively.

The mechanism of tool wear in metal cutting is complicated and involves abrasive, adhesive, and diffusion wear. The specific impact of each of them depends from material properties, tool, workpiece, and processing conditions. Testing the wear resistance of HSS is performed using "ball/disk" or rolling contact tribological testing procedures.

Figure 7 shows the wear-rate (mm^3/Nm) of HSS samples after the test scheme "ball/disk." You can see that all nitrided samples show a significant decrease in the wear-rate compared to the initial condition. The wear-rate of R9, R6M5, and R18 HSS nitrided samples is reduced by 77%, 81%, and 83%, respectively, which indicates a significant increase in HSS wear-resistance after nitriding.

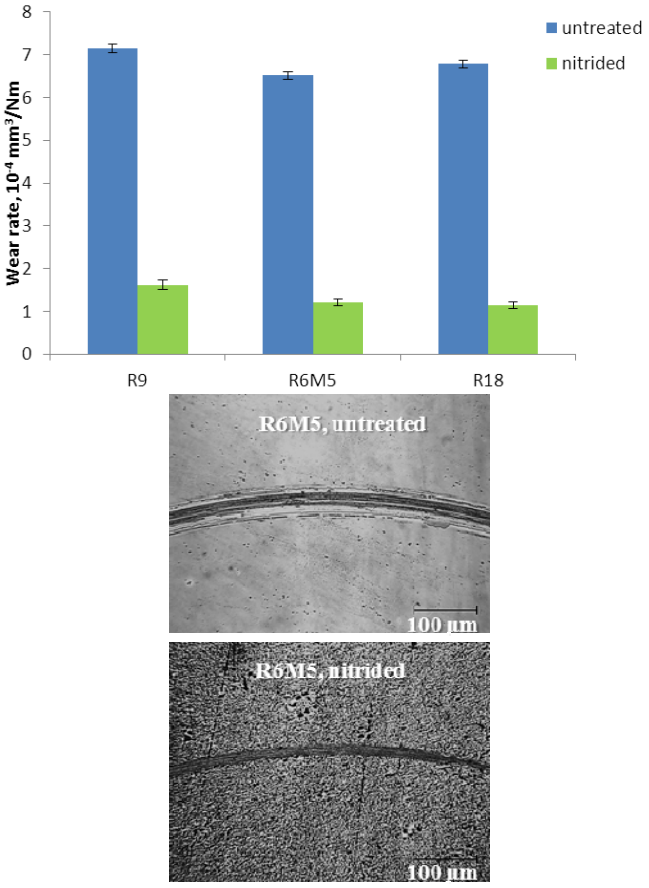

Fig. 7. Wear rate of the untreated and electrolytic-plasma nitrided HSS samples
Rys. 7. Intensywność zużywania nieobrobionych i azotowanych elektrolitycznie-plazmowo próbek HSS

The results of sample tests for abrasive wear indicate the weight loss after the wear process. Figure 8 shows the values of weight loss for R9, R6M5, and R18 steels before and after nitriding. The results indicate that the weight loss of the nitrided samples was less than untreated samples, indicating improved resistance of HSS to abrasive wear after nitriding. The resistant to abrasive wear of R6M5, R18 steels before and after nitriding is a little higher than R9 steel. Because R9 steel characterized by fewer solid carbide, alloying elements and fine nitrides of alloying elements. It is known **[L. 16–18]** that the nature, quantity, distribution, and carbides size has a significant influence on the wear-resistance of HSS. In addition, for the protection of grain volume, a relatively mild matrix from abrasion is needed to disperse fine nitrides of alloying elements.

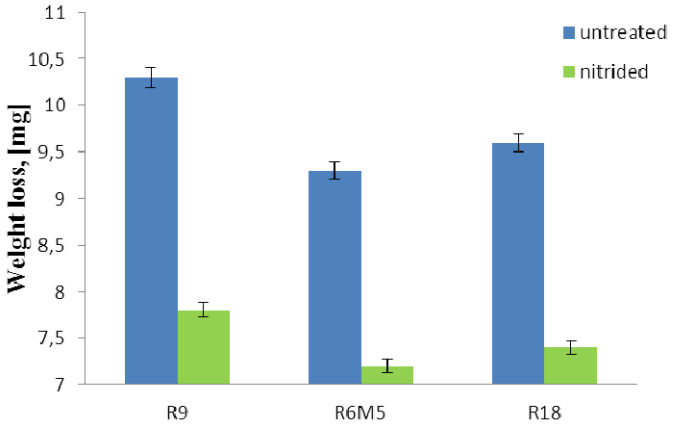

Fig. 8. Figures of the mass wear of the R9, R6M6 and R18 steels before and after nitriding
Rys. 8. Wartości zużycia masowego stali R9, R6M6 i R18 przed i po azotowaniu

Thus, it is established that the surface layers of the HSS samples had a higher wear-resistance as a result of electrolytic-plasma nitriding. The increase of wear-resistance after nitriding is mainly due to the formation of a nitrogen martensite diffusion layer with Fe_4N (γ'-phase) monophasic nitride. In addition, the inclusion of fine nitrides of alloying elements had a substantial influence on wear resistance. A significant increase of HSS wear-resistance after electrolytic-plasma nitriding shows the prospects of using this method for improving the performance of cutting tools.

CONCLUSION

Analysing the obtained results, we can make the following conclusions:

1. We determined that fine inclusions of an average size ~0.1 μm after electrolytic-plasma nitriding on the surface of investigated HSSs are formed. It is assumed that these fine inclusions are finely dispersed inclusions of alloying elements nitrides.
2. It is experimentally established that, on a surface of steels R9, R6M5, R18 after electrolytic-plasma nitriding at 550°C, a nitrided layer consisting of the diffusion layer with Fe_4N monophasic nitride (γ'-phase) is formed.
3. We determined that the intensity of wear of the nitrided samples of R9, R6M5, and R18 HSSs are reduced by 77%, 81%, and 83%, respectively, which indicates a significant increase in the wear-resistance of HSS after electrolytic-plasma nitriding.
4. It was found that there are increases in the resistance to abrasion of tool steels after electrolytic-plasma nitriding. The increase of wear-resistance after electrolytic-plasma nitriding is mainly due to the formation of a diffusion

layer of nitrogen martensite with Fe_4N (γ'-phase) monophasic nitride on the surface.

Acknowledgement

This work was supported by the Committee of science of RK in 2013-2015 program „Grant funding for research".

REFERENCES

1. Vereshhaka A.S., Rabotosposobnost' rezhushhego instrumenta s iznosostojkimi pokrytijami. – M.: Mashinostroenie, 1993. – 336 s. [In Russian]
2. Grigor'ev S.N., Tehnologicheskie metody povyshenija iznosostojkosti kontaktnyh ploshhadok rezhushhego instrumenta [Tekst]: Monografija / S. N. Grigor'ev; V.P. Tabakov, M.A. Volosova. – Staryj Oskol: TNT, 2011. – 379s. [In Russian]
3. A. da Silva Rocha, T. Strohaecker and T. Hirsch, Effect of different surface states before plasma nitriding on properties and machining behavior of M2 high speed steel, Surface and coatings technology, 165 (2003), pp. 176–185.
4. U. Ion-Dragos, H. Iosif, S. Viorel-Aurel, Microstructure and abrasion wear-resistance of thermally sprayed cermet coatings, Materials testing 55 (2013), No.1, pp. 47–50.
5. Struktura i iznosostojkost' azotirovannyh stalej / S.A. Gerasimov, L.I. Kuksenova, V.G. Lapteva, Je.A. Eliseev: Uchebnoe posobie. -M.: Izd-vo MGTU im.N.Je.Baumana, 2002. -48 s. [In Russian]
6. Duradzhi V.N., Himiko-termicheskaja obrabotka metallov s nagrevom v jelektrolitnoj plazme // Actual Conference. Tehnologii obrabotki poverhnosti, 6 (69), 2010 g – s. 45–50. [In Russian]
7. Gupta P., Tenhundfeld G., Daigle E.O., Ryabkov D., Electrolytic plasma technology: Science and engineering – an overview // Surf. &Coat. Technol. 2007. V. 25. P. 87–96.
8. Suminov I.V., Belkin P.N. i dr. Mir materialov i tehnologij. V 2-h tomah, Tom 1, M. izd. Tehnosfera, 2011, – 464 s. [In Russian]
9. Gol'dshtejn M.I., Grachev S.V., Veksler Ju.G., Special'nye stali. – M.: Metallurgija, 1985. – 408 s. [In Russian]
10. Struktura i iznosostojkost' azotirovannoj stali /L.I.Kuksenova, V.G.Lapteva, E.V. Berezina i dr. //MiT()M.-2004. -№1. -S.31 34. [In Russian]
11. Lahtin Ju.M., Kogan Ja.Je., Shpis G.I., Bener 3. Teorija i tehnologija azotirovanija.- M.: Metallurgija, 1991 g. 320 s. [In Russian]
12. Novye idei o mehanizme obrazovanija struktury azotirovannyh stalej /S.A. Gerasimov, A.V. Zhiharev, E.V. Berezina, G.I. Zubarev //MiTOM,- 2004. № 1. – S. 13–17. [In Russian]
13. Arzamasov B.N., Bratuhin A.G., Eliseev Ju.S., Panajoti T.A., Ionnaja himiko-termicheskaja obrabotka splavov. M., izd-vo MGTU im.N.Je. Baumana, 1999, 400 s. [In Russian]

14. Skakov M.K., Rakhadilov B.K., Sheffler M., Modification of structure and properties of steel R6M5 at electrolyte plasma treatment // Advanced Materials Research / Vol. 601, 2013 – pp. 64–68.
15. Kremnev L.S., Teorija legirovanija i sozdanie na ee osnove teplostojkih instrumental'nyh stalej i splavov / Metallovedenie i termicheskaja obrabotka metallov №11 (641), 2008 – P. 18–27.
16. Badisch E., Mitterer C. // Tribology International. 2003. V. 36. N 10. P. 765−770.
17. Gnjusov S.F., Hazanov I.O., Sovetchenko B.F. i dr. Primenenie jeffekta sverhplastichnosti stalej v intrumental'nom proizvodstve. Tomsk: NTL, 2008. 240 s.
18. Chaus A.S., Hudakova M. // Wear. 2009. V. 267. P. 1051−1055.

Streszczenie

Zbadano wpływ azotowania elektrolityczno-plazmowego na strukturę i własności tribologiczne stali szybkotnących (HSS) typu R9, R6M6 i R18. Wykazano, że po takiej obróbce w temperaturze 550°C tworzona jest warstwa azotowana zawierająca monofazowy azotek Fe_4N (faza γ'). Taka warstwa azotków ma wysoką odporność na zużywanie z jego intensywnością zredukowaną do 1/6 wartości dla próbek niepoddanych obróbce.